



An evaluation of ear biometric system based on enhanced Jaya algorithm and SURF descriptors

Partha Pratim Sarangi¹ · Bhabani Shankar Prasad Mishra² · Satchidanand Dehuri³ · Sung-Bae Cho⁴

Received: 8 November 2018 / Revised: 30 September 2019 / Accepted: 27 October 2019 / Published online: 9 November 2019
© Springer-Verlag GmbH Germany, part of Springer Nature 2019

Abstract

Recently, the ear biometric has received much attention for human recognition due to its unique shape and rich local features. However, extracting discriminative features from ear images is a crucial task in presence of illumination changes, low contrast, noise, and pose variations. With the aim of neutralizing the effect of these factors, this paper proposes an automatic enhancement technique using meta-heuristic optimization to enhance the ear images. Here, we modified a recent and simple yet meta-heuristic optimization technique known as Jaya algorithm by introducing a mutation operator to enhance the ear images in few iterations and the proposed approach is named as enhanced Jaya algorithm. Then, we employed a pose-invariant local feature extractor, SURF to extract local features. Finally, the k -NN classifier has used to evaluate the rate of correct identification. Extensive experiments are conducted on four standard datasets and the performance evaluation is carried out by qualitative and quantitative measures. Experimental results clearly indicate the proposed enhancement approach is competitive as compared to two classical methods HE, CLAHE, and two meta-heuristic algorithms PSO and DE-based image enhancement techniques.

Keywords Image enhancement · Ear biometrics · Ear identification · Jaya algorithm · Speeded-up robust features

1 Introduction

In the last decades, biometric systems are being widely used as a major domain of security applications in the electronically advanced society. It has led to the development of many biometric systems using different biometric traits. Among numerous biometric traits, the ear shape has become a very much popular and well-accepted biometric trait for human recognition owing to its unique shape, stable structure, and salient features. In addition, the ear biometric is a good alternative to other successful physiological modalities including

fingerprint, iris, and palmprint because it is non-intrusive and less cooperation is needed from the users for recognition operation. This biometrics requires a low expensive camera to capture 2D ear images like face biometric trait but having promising recognition performance than face. Again, as size of ear shape is smaller, it can easily combine with other biometric trait to overcome the problems of unimodal biometric systems.

In 1890, first-person Alphonse Bertillon suggested that the shape of the outer ear can be used for human identification. After a long duration in 1989, the American police officer Alfred Iannarelli [21] developed a manual measurement based ear identification system. He performed extensive experiments on ten thousand ear images based on twelve unique features or measurements of ear for identification of different shape of the ears. During latter part of 20th century, Burge and Burger [6] were the first to propose a computer based ear biometric system. With the intention of studying the uniqueness of the ear prints, one project the Forensic Ear identification (FearID) was commenced by nine institutes from Italy, the UK and the Netherlands in 2006. The outcome of their study brought to the public with the conclusion that earprints can be used as biometric

✉ Partha Pratim Sarangi
ppsarangi@gmail.com

¹ Department of Computer Science and Engineering,
Seemanta Engineering College, Jharpokharia, Mayurbhanj,
India

² School of Computer Engineering, KIIT University,
Bhubaneswar, India

³ Department of Information and Communication Technology,
Fakir Mohan University, Balasore, India

⁴ Soft Computing Laboratory, Department of Computer
Science, Yonsei University, Seoul, Korea

in a semi-automated identification system. Since then, ear biometrics has been deployed in many areas including identity recognition, surveillance, law enforcement, and forensics applications [16].

However, ear biometrics based on 2D ear images still undergo poor recognition performance due to improper acquisition such as poor contrast, blur, illumination variations, and noise. Various enhancement techniques are generally used to resolve the above problems occurring at the time of capturing the 2D ear images. In the biometric systems, contrast enhancement step is very important towards improvement of recognition performance. This enhancement operation can be broadly classified into two categories such as spatial domain and frequency domain. The most commonly used enhancement techniques of the spatial domain are classified into four types based on the operation performed on the pixels of the image such as pixel-wise operation [42], filter operation [18, 41], transformation [42], and multi-scale enhancement [25]. The linear contrast enhancement, gamma correction are the example of pixel-wise enhancement. The proposed image enhancement approach in this paper is based on filter operation. All histogram based enhancement approaches are based on transformation operation.

In order to reduce the effect of low contrast from 2D images the following enhancement techniques are widely used such as histogram equalization (HE) [42], and contrast-limited adaptive histogram equalization (CLAHE) [36]. In HE, the intensity of each pixel of the image is modified based on relative frequency of the intensity of every pixels. Due to this both object and background are equally enhanced, which tends to introduce noise in the background. It also over-enhances the image contrast in presence of high peaks in the histogram. Unlike evaluating a single histogram for the entire image, the AHE enhancement technique divides the image into a number of tiles and computes histograms of each region to redistribute the intensity values of these regions. Finally, the enhanced intensity values of the neighboring tiles are combined using bilinear interpolation to obtain the entire image. The main benefit of AHE is the enhancement of local detail information contents and noise enhancement is still a problem. To minimize the noise, the CLAHE introduced one extra step clipping the height of the local histograms before the computation of its CDF. In CLAHE, histogram clipping step does not fully assure to eliminate noise. In addition, the selection of the clipping limit is image dependent.

Unlike traditional image enhancement techniques, recently many meta-heuristic optimization algorithms are deployed to search for the optimal parameters of the transfer function which maps the intensity values of the pixels into enhanced intensity values of the input image. Gorai et al. [18] proposed an approach based on particle swarm

optimization (PSO) [14, 28] which gave promising results on the standard images. Similarly, Sarangi et al. [41] explored differential evolution (DE) [11, 43] to enhance the standard images which also gave promising results. Recently, many meta-heuristic algorithms [12] have been studied to obtain optimal parameters value of the transformation function, but most of them suffer from large computational times and proper tuning of the algorithmic-specific parameters to achieve better performance.

The main contribution of our paper is to develop an automated image enhancement approach in order to resolve the above mentioned issues in the existing enhancement methods. Initially, enhanced Jaya algorithm (EJA) has been exploited to enhance contrast level of the ear images in the preprocessing stage of the ear biometric system in less computation overhead. The enhanced ear images contain more detail information that allows extracting rich features in order to improve recognition performance. In the next stage, we employed a local feature extractor, the Speeded-up Robust Features (SURF) has been employed to extract the most discriminant local descriptors under pose variations. Finally, the nearest neighbor classifier is trained using minimum training set including two samples per each subject for person identification in the matching stage.

The rest of the paper is organised as follows. Section 2 describes background study of the problem. Detail description of ear biometric system and a review of existing works available for ear localization and recognition in Sect. 3. Section 4 presents the proposed ear biometric system. A comprehensive analysis of the experimental results of proposed approach is compared to the results of two classical approaches and two meta-heuristic approaches of ear images enhancement in Sect. 5. Section 6 emphasizes conclusion and future scope.

2 Problem formulation

Image enhancement is one of the important tasks in the preprocessing module of a biometric system. The main objective of an efficient image enhancement algorithm is to highlight the fine detail contents of the input image which can easily separate the object from the background. Hence, enhanced image can be utilized to extract more discriminating features that improves recognition performance of the biometric system. The proposed image enhancement technique is based on a spatial operation or filter operation which is performed using two functions. First, the transformation function is used to modify the pixel intensity values based on both statistical global and local information and four parameters. Second, the fitness or cost function is required to estimate the information content of an image.

The mathematical expression of the transformation function and fitness function are given in the following subsections.

2.1 Transformation function

Transformation function updates the pixels intensity values to new intensity values based on Eq. (1) derived from global and local statistical information of the input image. To extract global statistical information, all the pixels’ intensity values of the image of dimension ($P \times Q$) are utilized. Similarly, for extracting local statistical information, it depends on the neighborhood pixels intensity values of a predefined ($n \times n$) window. The mathematical form of the parametric transformation function $g(p, q)$ for both global and local enhancement is derived as follows:

$$g(p, q) = K(p, q) * [f(p, q) - c.\mu(p, q)] + \mu(p, q)^a \tag{1}$$

where $K(p, q)$ is known as image enhancement function, which is expressed using the global mean (M) and local standard deviation (σ) in Eq. (2). Similarly, $\mu(p, q)$ and $\sigma(p, q)$ denote the local mean and local standard deviation of the current pixel, which is calculated using ($n \times n$) neighborhood pixels intensities centred around current pixel (p, q). Image enhancement function, global mean, local mean, and local standard deviation of an image $f(p, q)$ are given in Eqs. (2), (3), (4) and (5) respectively.

$$K(p, q) = \frac{k.M}{\sigma(p, q) + b} \tag{2}$$

$$M(p, q) = \frac{1}{p \times q} \sum_{p=1}^P \sum_{q=1}^Q f(p, q) \tag{3}$$

$$\mu(p, q) = \frac{1}{n} \sum_{i=1}^n \sum_{q=1}^n f(p, q) \tag{4}$$

$$\sigma(p, q) = \left(\frac{1}{n} \sum_{p=1}^n \sum_{q=1}^n (f(p, q) - \mu(p, q))^2 \right)^{\frac{1}{2}} \tag{5}$$

Finally, Eq. (1) can be rewritten by substituting Eqs. (2) in (1) to get the required transformation function as:

$$g(p, q) = \frac{k.M}{\sigma(p, q) + b} [f(p, q) - c\mu(p, q)] + \mu(p, q)^a \tag{6}$$

The transformation function in Eq. (6) enhances the contrast level of the input image centred at the local mean. The four positive real-valued parameters (a, b, c, k) of the transformation function decides the intensity values of the enhanced image. Since these four parameters play an important role to vary the contrast level of the input image over a broader

range. Hence, the proposed enhancement technique optimizes those four parameters value over the predefined ranges of the transformation function to enhance the intensity values of the input image.

2.2 Evaluation of fitness function

In order to measure the amount of enhancement of an enhanced image, an fitness function is used after assigning a specific parameters values of $a, b, c,$ and k on the transformation function. The higher fitness value of an enhanced image indicates more enhancement has acquired. Designing a good fitness function, it depends on measurement parameters used. In general, the enhanced image maximizes a number of edges and entropy in comparison with the input image. An enhanced image expands the gray-levels over a wide range which increases the details edge information. Similarly, the entropy increases due to enhancement of intensity of the pixels in the enhanced image. In this work, the fitness function is used for the proposed approach is sum of edge intensities, number of edge pixels (edgels), and entropy of the enhanced image. These three evaluation measures are combined to define an effective fitness function. An effective fitness function should be chosen to measure the fitness value of the enhanced image. This leads to an increase in entropy value because of more information present in the enhanced image [8]. The fitness function is presented in the form of equation as follows:

$$F(I_{enhanced}) = \log(\log(E(I_{edge}))) \times \frac{edgels(I_{edge})}{M \times N} \times H(I_{enhanced}) \tag{7}$$

where $I_{enhanced}$ is the enhanced image obtained from the transformation function in Eq. (6) and I_{edge} is the edge image obtained from Sobel edge detection. The edgels (I_{edge}) is the number of edge pixel in the edge image of enhance image. $E(I_{edge})$ the is sum of all the pixel intensity values of the enhanced image which is corresponding to edge pixels of the edge image and $H(I_{enhanced})$ is the entropy value of enhanced image. $E(I_{edge})$ is calculated as follows:

$$E(I_{edge}) = \sum_{p=1}^P \sum_{q=1}^Q I_{enhanced} * I_{edge} \tag{8}$$

The entropy of the enhanced image $I_{enhanced}$ determines the information content which is calculated as follows:

$$H(I_{enhanced}) = - \sum_{i=0}^{L_{max}-1} p(i) * \log_2(p(i)) \tag{9}$$

where $p(i)$ indicates the probability of occurrence of pixels with gray level $i \in (0, L_{max} - 1)$ and L_{max} indicates the maximum gray level present in the enhanced image ($I_{enhanced}$).

2.3 Jaya algorithm and enhanced Jaya algorithm

All meta-heuristic optimization approaches are randomized algorithms which need controlling parameters to control the path of the candidate solutions towards a global optimal solution. Thus, these algorithms require proper tuning of the control parameters to guide candidate solutions to converge at global optimal solution. Among all meta-heuristic algorithms, Jaya algorithm does not need algorithm-specific control parameters. This subsection provides an in-depth description of Jaya algorithm (JA) and the proposed enhanced Jaya algorithm (EJA).

2.3.1 Jaya algorithm

Jaya algorithm (JA) [35] is a recent and simple yet meta-heuristic algorithm introduced by Venkata Rao. The name Jaya algorithm has originated from Sanskrit language, meaning of the word Jaya is victory. The principle behind this algorithm is always getting the optimal solution by following best and avoiding the worst solutions. However, it is parameters free, this key fact makes JA popular among many researchers. In recent years, it has been used in various optimization problems in different domains of engineering applications [29, 44, 47, 48].

JA utilizes two operators such as selection and updating the candidate solutions. After selection of best for each candidate solution from the present solution and the next solution based on their fitness values. JA relies on the present best and worst solution to update each individual solution for the next generation. At each generation, the candidate solutions are updated to move toward a global optimal solution with the principle of following the best and avoiding the worst solutions. Mathematical expression [35] for updating candidate solutions are as follows:

$$X_{i,j}(g+1) = X_{i,j}(g) + r_{1,i,j} * (X_{i,best}(g) - |X_{i,j}(g)|) - r_{2,i,j} * (X_{i,worst}(g) - |X_{i,j}(g)|) \quad (10)$$

where $X_{i,j}(g)$ is the value of the j th parameter for i th solution at iteration g , $X_{i,best}(g)$ and $X_{i,worst}(g)$ is the value of the i th parameter for the best solution and the worst solution at iteration g respectively, $r_{1,i,j}$ and $r_{2,i,j}$ are two random numbers generated in the range of [0, 1] at iteration t , finally $X_{i,j}(g+1)$ represent the updating value of j th parameter for i th candidate solution in the next iteration ($g+1$). Continuous upgrading every candidate solution at next iteration using Eq. (10) exploits neighborhood positions that leads to converge at global solution. In addition, two random numbers $r_{1,i,j}$ and $r_{2,i,j}$ enhance the exploration capability of Jaya algorithm.

After updating the candidate solutions at current iteration n , then the selection process is used to select the best individual solution between the current solution $X_j(g)$ and the updating next solution $X_j(g+1)$ based on fitness values for the next iteration ($g+1$) which is described in [35] as follows:

$$X_j(g+1) = \begin{cases} X_j(g), & \text{if } f(X_j(g)) > f(X_j(g+1)) \\ X_j(g+1), & \text{otherwise} \end{cases} \quad (11)$$

As a result, all candidate solutions of the next iteration are best than their corresponding solutions in the current iteration. In accordance with the selection of the candidate solutions for next iteration, all their fitness function values are modified and considered as the input to next iteration.

2.3.2 Enhanced Jaya algorithm

One major issue of Jaya algorithm is slow convergence to the global best solution. In order to achieve fast exploration and convergence to optimal solution, we incorporate an efficient mutation strategy in the Jaya algorithm to avoid slow convergence and it is termed as the enhanced Jaya algorithm (EJA). In the experimental evidence, the combination of mutation operator with Jaya algorithm can enhance the candidate solutions diversity and searching capability. As a result, the mutation operator increases the convergence rate that leads to reach at the optimal solution in less iterations.

As mentioned in [41], DE outperforms the PSO based image enhancement in terms of performance and faster convergence to the global optimal solution. In each generation, DE executes mutation operation for the entire population before crossover and selection operations. Hence, DE can explore the search space faster than other existing evolutionary algorithms. However, it takes high computational time for execution and occasionally, its performance degrades in case of stagnation of the population that leads to premature convergence or slow convergence to the optimal solution. For this reason, we randomly incorporated the mutation operator of DE in the Jaya algorithm to enhance diversity in the solutions after performing updating and selection operations on the candidate solutions. In the proposed EJA, we used an adaptive selection of the mutation operator to balance exploitation and explorations in less computation time. This mutation operator mathematically expressed as

$$X_j(g+1) = X_{r_1}(g) + F * (X_{r_2}(g) - X_{r_3}(g)) \quad (12)$$

where $j \in \{1, 2, \dots, K\}$, j th candidate solution of the population of size K . Similarly, r_1 , r_2 , and r_3 are the indices of the candidate solutions from $\{1, 2, \dots, K\}$. The n th and $(n+1)$ th represents solutions of the current and next iterations. F is the scaling factor lies in the range of [0,1] to control the difference vector in the mutation operation and avoid stagnation in the population. In this work, we have used an adaptive scaling factor which is described as

$$F = I + rand * ((G_{max} - g)/G_{max}) \tag{13}$$

where I is the initial value of scaling factor F which is 0.8, g is the current iteration and G_{max} is the maximum iteration. In addition, we can also adaptively evaluate the rate of mutation in Eq. (14) and the mutation operation will be performed when uniformly generated a random real number is greater than and equal to the rate of mutation.

$$rand(0, 1) \geq \left(1 - \frac{g}{G_{max}}\right) \tag{14}$$

The mutation rate varies from 1 to 0 in the successive iterations. Initially, the rate of mutation operation is less and gradually it increases in the last part of the iterations. In this way, it enhances the exploration capability of the algorithm. Finally, EJA balances both exploitation and exploration capability using upgrading and mutation operators.

2.4 Speeded-up robust feature transform (SURF)

An efficient local feature descriptors, named Speeded-Up Robust Features (SURF) proposed by Herbert Bay and his colleagues [4]. SURF detects scale and in-plane rotation-invariant interest points (key points) and its corresponding descriptors are generated. It provides a better result in computationally quite faster than another proficient local feature descriptor Scale Invariant Feature Transform (SIFT). In order to make all computations faster, integral images and Hessian matrix are used to detect interest points. The interest points are the blob-like structures at regions where the determinant of the Hessian is maximum. In an integral image I for a given point x with coordinate $x[p, q]^T$ the hessian matrix $H(x; \sigma)$ at scale σ is defined as:

$$H(x; \sigma) = \begin{bmatrix} L_{xx}(p, \sigma) & L_{xy}(p, \sigma) \\ L_{yx}(p, \sigma) & L_{yy}(p, \sigma) \end{bmatrix} \tag{15}$$

where $L_{xx}(p, \sigma)$, $L_{xy}(p, \sigma)$, $L_{yx}(p, \sigma)$ and $L_{yy}(p, \sigma)$ are the convolution of the Gaussian second order derivatives $\frac{\delta^2}{\delta x^2}g(\sigma)$, $\frac{\delta^2}{\delta x \delta y}g(\sigma)$, $\frac{\delta^2}{\delta y \delta x}g(\sigma)$ and $\frac{\delta^2}{\delta y^2}g(\sigma)$. The computation of the Hessian matrix is expensive and time consuming. Hence, Hessian can be computed approximately using box filters. For scale invariant, SURF uses a pyramidal scale space, like SIFT. But, it is different from SIFT; the SURF can directly change the scale because of the box filters and integral image. The scale space is analysed by up-scaling the filter size of a certain dimensions (9×9 , 15×15 , 27×27 , etc.). The key-points are localized in the image and over scales; a non-maximum suppression in a $3 \times 3 \times 3$ neighborhood is applied. Then, the descriptor is calculated for all interest points by considering a circular region near the interest points and the sum of Haar wavelet responses in horizontal (dx) and vertical (dy) directions are computed. In order to make descriptors rotation invariant, an orientation selection

method has introduced in [4]. The square region is divided into 4×4 grids to preserve spatial information. For each subdivision, authors computed the horizontal and vertical Haar wavelet responses at 5×5 equally spaced sample points. The sum of the wavelet responses in dx and dy for each subdivision is used as first set of entries in feature descriptor. In addition, the sum of absolute values of the responses, $|dx|$ and $|dy|$ are computed to obtain the information about the polarity of the intensity changes. Hence, for i th subdivision the feature descriptor V_i is given by

$$V_i = \{\Sigma dx, \Sigma dy, \Sigma |dx|, \Sigma |dy|\} \tag{16}$$

These local feature descriptors (V_i) are concatenated to form a 64 dimensional feature descriptor which expresses the interest point and nearest neighbors. Next, feature descriptor of the interest points are matched. In our work, matching of descriptors can be done by three distance measures such as Euclidean distance (d_1), Canberra distance measures (d_2), nearest neighbor distance ratio (d_3). The distance between two descriptors D_1 and D_2 using Euclidean distance is given by

$$d_1 = \sqrt{\sum_{i=1}^{64} (D_{1i} - D_{2i})^2} \tag{17}$$

$$d_2 = \sum_{i=1}^{64} \frac{|D_{1i} - D_{2i}|}{|D_{1i}| + |D_{2i}|} \tag{18}$$

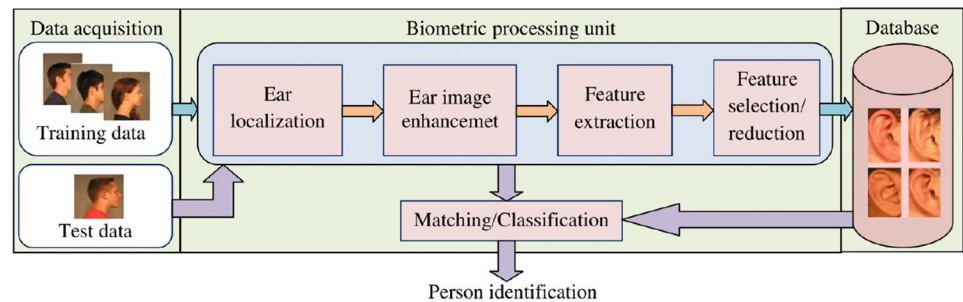
$$d_3 = \frac{d_1(D_1, D_2)}{d_1(D_1, D_3)} < \theta \tag{19}$$

If nearest neighbor ratio in Eq. (19) is less than θ , then (D_1, D_2) descriptors have better match, otherwise they have no match. In our experiments, in most of the cases Euclidean distance metric in Eq. (17) outperforms than Canberra distance in Eq. (18) and nearest neighbor distance ratio in Eq. (19).

3 Generic ear biometric system

A biometric system works in two phases: one ear enrolment phase and second ear recognition phase. In the enrolment phase, the biometric system is trained using multiple images for each person and all the feature sets of the individuals are stored in the database. Similarly, in the recognition phase, an individual is recognized by the biometric system. A generic ear recognition system is as shown in Fig. 1, which is basically consists of four modules: ear localization, ear image enhancement, feature extraction, and matching/classification. First module is the ear localization module in which the ear shape is localized and cropped from the side face image. The input ear image may be affected by low contrast, illumination variation, and noise which influences the recognition performance through

Fig. 1 The generic ear recognition system



misclassification. Hence, the second module is the image enhancement in which the quality of the ear image is enhanced to extract discriminative features in the feature extraction module. The feature set of the enhance ear image can be generated using global or local feature extraction technique. As the feature set contains redundant features, it is necessary to select unique features or discriminant features using either feature selection or reduction technique. Then, the reduced feature set is used for person recognition in the recognition module.

Various ear localization and recognition approaches have proposed in the literature, we describe a review of some recent and well-known approaches of ear localization and recognition in 2D images. Yuan et al. [51] have employed skin-colour and elliptical contour information for ear localization. Ibrahim et al. [22] utilized a bank of curved and stretched Gabor wavelets known as banana wavelets, which is similar to ear structure used for ear localization. Islam et al. [24] proposed an Adaboost technique which yields huge time for ear localization. Prakash et al. in [33] presented a template matching based ear localization technique in which template has been resized according to the size of the side face to make it suitable for each test images. Prakash et al. [34] used hierarchical clustering of the edge map to localize ear. Prakash et al. [31] utilized connected components of a graph from the edge map and selected a set of connected component as probable ear candidates. Recently, we have efficiently used modified Hausdorff distance for ear localization. Sarangi et al. [39] presented a new scheme of automatic ear localization based on template matching with the modified Hausdorff distance. Recently, Emeršič et al. [17] proposed a novel ear detection technique based on convolutional encoder-decoder networks (CEDs).

In the literature, ear recognition methods can be categorized into the five categories: holistic approaches, structural approaches, spectral approaches, local descriptor-based approaches, and deep learning approaches. The holistic approaches use statistical measures which are evaluated from the image as a whole. Victor et al. [46] applied principal component analysis (PCA) method on the training ear images to compute eigenvectors and test ear images are projected on the basis eigenvectors for ear recognition. Zhang et al. [52] proposed an ear recognition system using a combination of independent component analysis (ICA) and a radial

basis function network (RBFN). Xie and Mu [49] proposed an improved locally linear embedding (IDLLE) algorithm for dimensionality reduction of multi-pose ear recognition using KNN classifier. The performance of improved LLE has improved over LLE, PCA and KPCA. Yuan and Mu [50] proposes ear recognition system based on sparse representation to deal with ear recognition under partial occlusion.

The structural approaches use ear shape and structure to recognize the persons. Burge and Burger [6] represented ear as an adjacency graph from the Voronoi diagram of its edge segments and novel graph matching algorithm has used for ear recognition. Hurley et al. [20] proposed a novel feature extraction technique, force field transformation for ear localization and recognition. Choras [9] has used geometric features to represent the ear shape for ear recognition.

The spectral approaches utilize different frequency spectrums to recognize the persons. Sana and Gupta [37] proposed an efficient ear biometric system in which authors used multi-resolution discrete wavelet transform (DWT). Kumar and Wu [27] utilized a log-Gabor based combination approach for ear identification. Abate et al. [1] proposed a rotation invariant descriptor technique for ear recognition using generic Fourier descriptor to extract features from ear images. Basit and Shoaib [3] proposed a ear recognition method based on discrete curvelet transform (DCT).

In the last decade, many researchers have published local features-based ear recognition techniques. The local features represent an image into multiple image patches or the keypoints which can characterize by multiple feature vectors or descriptors. As a result, the descriptors contain detail local information which is more robust to occlusion or clutter. Many researchers have explored well-known single local feature or fusion of multiple local features representation to improve recognition performance in the ear biometric systems under illumination, pose, scale variation, partial occlusion, and clutter. Guo et al. [19] presented a texture based local feature called Local Similarity Binary Pattern (LSBP). Bustard and Nixon [7] considered ear image as a planar surface and created a homography transform using SIFT feature points to register ears accurately. Damer and Führer [10] used multi-scale dense HOG features, Pflug et al. [30] utilized local phase quantization (LPQ) descriptor, Benzaoui et al. [5] employed binarized statistical

Fig. 2 Block diagram of the proposed ear biometric system

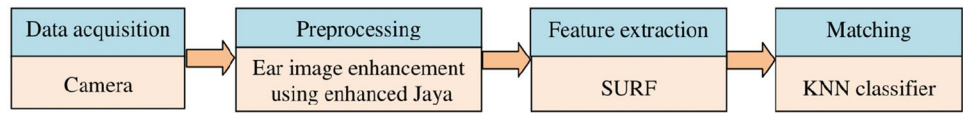


image features (BSIF), and Sarangi et al. [38] explored pyramid histogram of oriented gradients (PHOG) as a descriptor of 2D ear shapes to extract discriminative features for ear recognition. Some authors tried to use multiple representations to increase the recognition performance namely, Badrinath and Gupta [2] performed feature-level fusion of different poses of ear images to form a fused template for ear verification; Kisku et al. [26] exploited scale invariant feature transform (SIFT) feature descriptors for the ear recognition; Prakash and Gupta [32] fused the speeded-up robust feature (SURF) on enhanced ear images; Sarangi et al. [40] proposed a feature-level fusion of two local features PHOG and LDP representation for each ear shape and reduced combined feature dimension using KDA.

Most recently, Emeršič et al. [15], Dodge et al. [13] and Zhang et al. [53] proposed CNN based ear recognition under uncontrolled conditions with illumination, pose, scale variations, partial occlusions, and clutter.

4 Proposed technique

Like other biometrics, the proposed ear biometric system consists of three main components: preprocessing, feature extraction, and matching. Figure 2 illustrates the major steps of the

proposed ear biometric system. The ear images can be easily captured using the low-resolution camera at a distance because of which it suffers from pose variation, illumination changes, partial occlusion, and clutter. After the acquisition of 2D side face image using the camera, the preprocessing module starts to localize ear shape from the side face image and then enhancement technique is used to improve the quality of the ear image. This preprocessing stage plays a vital role in the improvement of recognition performance. The enhancement technique increases the discriminant features contained in the original ear image that leads to improve the recognition performance. We have explored a new and simple yet meta-heuristic optimization algorithm known as Jaya algorithm which does not require algorithmic-specific control parameters and only one updating operation (10) is used for exploitation and exploration operations. In our work, we have used proposed enhanced Jaya algorithm (EJA) to improve the diversity in the search space by introducing the superiority of Differential evolution’s mutation operator in the simple Jaya algorithm. To examine the effectiveness of the enhancement approach, we use SURF feature extraction technique to make our algorithm robust to handle scale, rotation invariant, and occlusion. Then, for simplicity, we use *k*-NN classifier for identification of subjects.

Algorithm 1 the proposed enhanced Jaya algorithm (EJA)

- 1: Randomly generate an initial population (X) of *N* candidate solutions with $X_{i,j} = x_{i,1}, x_{i,2}, \dots, x_{i,d}, i = 1, \dots, N$ and $j = 1, \dots, d$ (number of parameters)
 - 2: Set current iteration *g* and maximum iterations G_{max}
 - 3: **for** $g \leftarrow 1$ to N **do**
 - 4: Enhance input image using transformation function using Eq. (6)
 - 5: Calculate fitness value F_i using Eq. (7)
 - 6: **end for**
 - 7: Obtain X_{worst} and X_{best} fitness values
 - 8: Find best solution, $X_{best_solution}$ w.r.t X_{best}
 - 9: **while** $g < G_{max}$ **do**
 - 10: **for** $i \leftarrow 1$ to N **do**
 - 11: Update candidate solution X_i using Eq. (10)
 - 12: Calculate fitness value F_{new_i} using Eq. (7)
 - 13: **end for**
 - 14: **for** $i \leftarrow 1$ to N **do**
 - 15: **if** $X_{new_i} > X_g$ **then**
 - 16: $X_i = X_{new_i}$
 - 17: **end if**
 - 18: **end for**
 - 19: Obtain X_{worst} and X_{best} fitness values
 - 20: Find the best solution, $X_{best_solution}$ w.r.t X_{best}
 - 21: **if** $rand(0, 1) \geq 1 - \frac{g}{G_{max}}$ **then**
 - 22: **for** $i \leftarrow 1$ to N **do**
 - 23: Perform mutation operation on X_i using Eq. (12)
 - 24: **end for**
 - 25: **end if**
 - 26: Increment the iteration count $g = g + 1$
 - 27: **end while**
 - 28: **return** optimal parameters (*a, b, c, k*)
-

The main advantage of our approach is that it does not need algorithmic-specific control parameters and we adaptively select mutation operation which makes it fully automatic ear enhancement technique. We used the proposed enhanced Jaya algorithm (EJA) for searching the optimal values of the parameters (a, b, c, and k) of the transformation function described in Eq. 6 in order to improve the quality of the input image. Experimentally, the upper and lower boundary of the four parameters has been fixed, which are given as follows: $a \in [0, 1.5]$, $b \in [1, \frac{gmean}{2}]$, $c \in [0, 1]$, and $d \in [0, 1.5]$. $X_{i,j}$ is the i th candidate solution with j th parameter in the population. $X_{i,j} = [0, 1, 0, 0]$ and $X_{i,j}^{th} = [1.5, \frac{gmean}{2}, 1, 1.5]$ are lower and upper bound of the parameters values of the candidate solutions. Algorithm 1 presents the basic steps of the proposed enhanced Jaya algorithm. All the candidate solutions of the population are randomly initialized using given formula as follow:

$$X_i = X_{i,j}^{low} + rand * (X_{i,j}^{high} - X_{i,j}^{low}) \quad (20)$$

Each candidate solution contains four parameters. They are randomly computed within a range of predefined search space based on the lower and upper bounds of each parameters. The population size N is set ten times the number of parameters which is 40 in our all enhancement experiments. After initialization of the population, the fitness function is used to evaluate the best and the worst solution of the population. Next, the fitness value for each solution evaluated in two phases. In the first phase, the transformation function in Eq. 6 used to modify the pixel values of the original image, and then in the second phase, the fitness value evaluated using Eq. 7 for enhanced image. In order to maintain diversity in the search space, the candidate solutions are updated using Eq. 10 to converge in the direction of the best optimal solution with the help of the best solution and the worst solution. Every solutions move towards an optimal solution by following best solution and avoiding the worst solution of each generation. This updating operation of the Jaya algorithm is merely responsible for exploitation and exploration in the search space. For this reason, the Jaya algorithm needs more number of iterations to reach near the best solution. Therefore, the proposed approach intended to introduce the mutation operation for improving diversity in the search space which reduces the number of iterations to converge the optimal solution. The mutation operation of DE algorithm is very much efficient to explore the search space. The same mutation operator in Eq. 12 has been employed in the proposed approach to improve diversity and fast convergence to the optimal solution. In this work, the mutation operator is applied to all candidate solutions of the specific iterations when a uniformly generated random number in the range of $[0, 1]$ is greater than $(1 - \frac{g}{G_{max}})$. It is observed that the probability of selecting mutation strategy depends on the

iteration index i.e. a few number of mutation operation have performed at the initial iterations and the probability of selecting mutation operation increases in the last stage of the iterations when the value of $(1 - \frac{g}{G_{max}})$ reduces from 1 to 0. Algorithm 1 describes the pseudo-code of the enhanced Jaya algorithm (EJA).

5 Experimental results

In this section, four different experiments of ear image enhancement are conducted to demonstrate the effectiveness of the proposed algorithm. First, the subjective evaluation of the original and enhanced images; second, SURF feature key-points matching; third, experiment is to examine the quantitative metrics such as detail variance (DV), background variance (BV), and edge counts; finally, evaluating the performance of the ear identification system based on enhanced ear images as inputs. The performance of the proposed image enhancement technique is compared to two classical well-known algorithms which are Histogram Equalisation (HE) and Contrast-Limited Adaptive Histogram Equalisation (CLAHE) and two popular meta-heuristic search algorithms such as Particle swarm optimization (PSO) and Differential evolution (DE) based image enhancement techniques, respectively. The experimental design and results are discussed in the following subsections.

5.1 Databases used

In this paper, all the experiments are carried out on the ear images from four widely used databases such as IIT Delhi (IITD) [23], University of Notre Dame collection E (UND-E) [45], collection J2 (UND-J2) [45], and the Annotated Web Ears (AWE) [16] standard databases. The IITD database contains ear images of the students and staff from the IIT Delhi, India. Recently, an extended version of ear database is available of 221 subjects with 793 images, where each subject age group varies from 14 to 58 years. In this database, most of the images are a very low contrast with large intra-class dissimilarity due to pose variation. Next, authors have selected two more databases from the University of Notre Dame (UND) such as collection E and collection J2 to handle more difficulties. The UND-E database contains 464 side face images from 114 subjects and 3–9 samples per subject. Images of the same subject are captured in different time with a large variation of pose and illumination effect. Similarly, The UND-J2 database consists of 2413 side face images taken from 415 subjects with 2–22 samples per subject. It can be noticed that most of the images have different objects in the background along with side face which is a challenging task to locate the ear region among multiple objects. In addition, female subject's images are

Table 1 Allocation of samples for training and test sets on four datasets

Datasets	Number of subjects	Training sample size	Testing sample size
IITD	221	442	221
UND-E	114	228	114
UND-J2	273	546	273
AWE	100	200	100

occluded by hair and earrings. Recently, an unconstrained ear images collected ‘in the wild’ of the ears of public figures collected by a web crawler named as AWE database. It consists of ten thousand ear images of 100 subjects with 10 samples per subject. In this database, images of the same subject have a huge variation in terms of illumination, pose, scale, and visual quality distortions. After ear localization all the ear images of four databases were resized for the enhancement and recognition as follows: IITD ear images resized $[50 \times 150]$, UND-E ear images resized $[80 \times 180]$, UND-J2 ear images resized $[80 \times 180]$, and AWE ear images resized $[100 \times 100]$ respectively.

In order to evaluate the performance of the image enhancement techniques, we perform identification operation comparisons on the enhanced images of each technique. In this experiment to determine the effectiveness of enhanced images of each database, we selected three samples for each subject from the database. Out of two samples are used as training samples and the remaining one is used as a test sample from every subject. In this way, three different combinations of datasets are built with two training samples and one test sample and an average of identification rates are determined for performance evaluation. The distribution of training and test samples of the four datasets are illustrated in Table 1.

5.2 Parameters Tuning

After ear localization operation, all the ear images were converted to the gray-scale images prior to the preprocessing operation. Then, low-pass filter was employed to minimize the illumination effect using the kernel or filter. Here, we experimentally determined different filter size for four databases such as for IITD kernel size is $[3 \times 3]$ for low resolution images, UND-E kernel size is $[11 \times 11]$ because most of the images are high contrast images, UND-J2 kernel size is $[5 \times 5]$, and AWE kernel size is $[7 \times 7]$. Next, for image enhancement many parameters of the classical PSO, classical DE, and proposed EJA have to be tuned to obtain optimal results i.e., to improve the contrast level of the ear images on the four databases. We have set experimentally the parameters of the PSO, DE, and EJA as mentioned in Table 2. As

Table 2 Parameters setting of PSO, DE, and proposed EJA for image enhancement

Classical PSO	Classical DE	Enhanced JA
Population size = 40	Population size = 40	Population size = 40
Max. Generation = 50	Max. Generation = 50	Max. Generation = 50
–	Scaling factor (F = 0.8)	Scaling factor (F = 0.8)
Inertia weight (W = 1.4)	–	–
Acceleration coefficients (C1 = 2.8, C2 = 1.4)	–	–
–	–	Adaptive mutation
–	Crossover rate C = 0.6	–

we know, the original Jaya algorithm is a parameter-free, simple, and computationally faster but it takes more generations to converge the optimal solution in comparison with DE and PSO. We have used adaptive mutation rate in the proposed approach when a real random value in the range $[0, 1]$ is greater than the mutation rate, then mutation operation is performed for all the candidate solutions of the population in that iteration. Unlike DE where mutation operation is performed in every generation, in EJA initially, more mutation operations are performed and gradually it reduces to zero in last generations. We introduced mutation operator in the Jaya algorithm to achieve higher exploration and fast convergence to optimal solution.

5.3 Performance measures

This section analyses experimental results of two classical and three meta-heuristic-based enhancement techniques on the four popular standard ear image databases. Two classical approaches are HE and CLAHE. Similarly, three meta-heuristic approaches are PSO, DE, and the proposed EJA. Figure 3 indicates the visual performance analysis of the enhanced sample images of our approach on the mentioned four databases. Figure 4 presents SURF key-points matching between original sample images and between enhanced images using our approach that indicates comparison of the enhanced images have more matching points on samples from four mentioned databases. Then, Figs. 5, 6, 7 and 8 show the visual presentation of sample images and their enhanced images obtained using HE, CLAHE, PSO, DE, and our EJA techniques on mentioned databases. Further, Figs. 9, 10, 11 and 12 indicate the rate of identification performance of four k -NN classifiers with four set of enhanced images obtained in preprocessing stage by using HE, CLAHE, and proposed EJA approaches. Tables 3, 4, 5, and 6 illustrate the quantitative performance measures

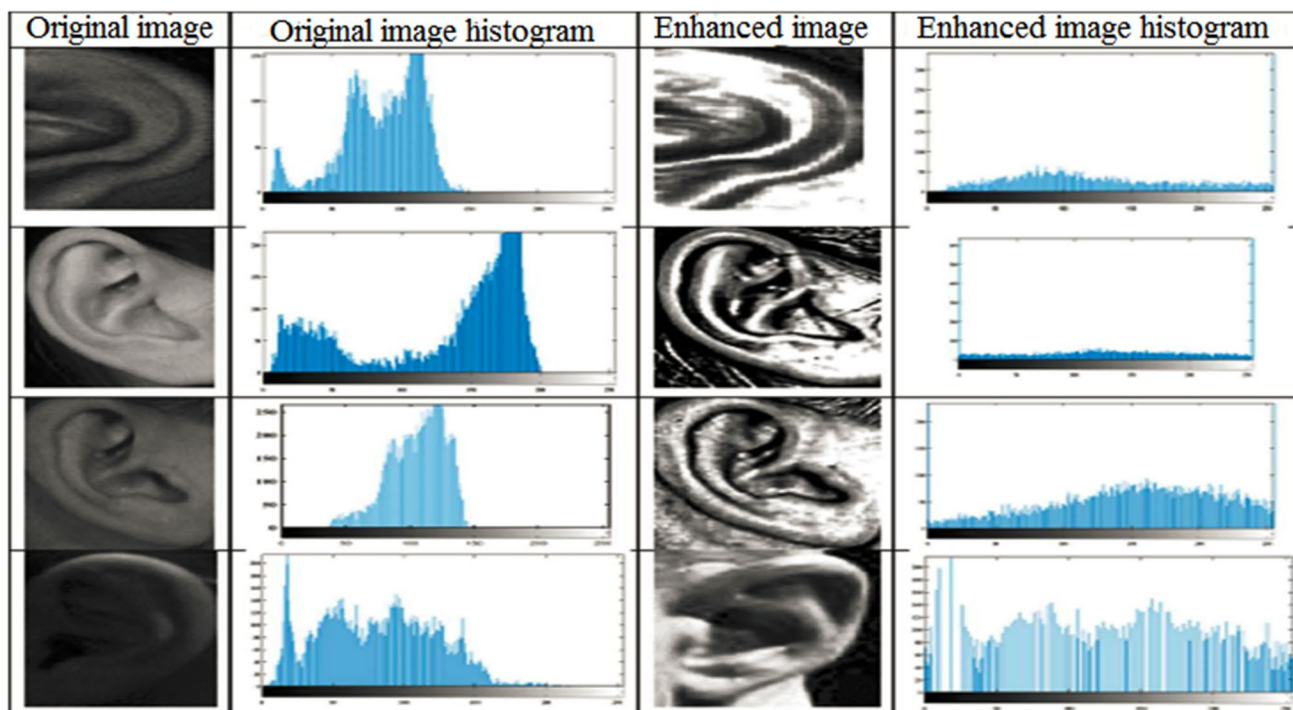


Fig. 3 Histogram based visual analysis of original and ours images

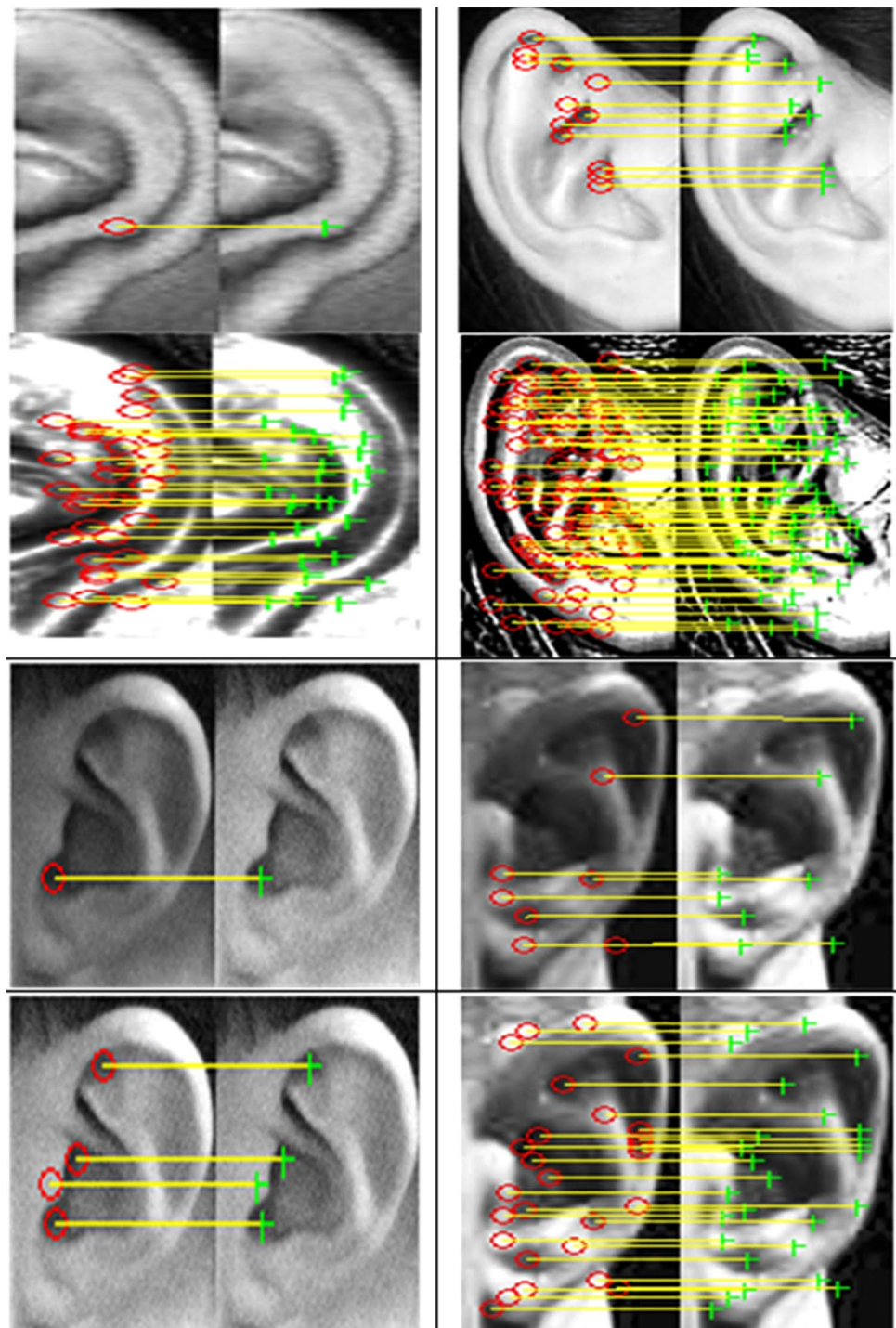
in terms of DV, BV, edge counts of four sample images on IITD, UND-E, UND-J2, AWE databases respectively. Similarly, Tables 7, 8, 9 and 10 give the rate of identification performance of the ear biometric systems based on HE, CLAHE, and EJA enhancement techniques used in pre-processing stage and ear image representation using SURF feature descriptors on IITD, UND-E, UND-J2, and AWE databases respectively.

At first, a subjective performance measure of the enhanced images is illustrated by using histograms of input and enhanced images. The histograms of the enhanced images are more flat or spread over the histogram of input images in the interval $[0, 255]$. Second, the performance measure based on SURF feature key-points matching, it counts a number of key points matched which is more in case of enhanced images. Third performance measure is a quantitative measure in which, we estimate detail variance (DV), background variance (BV), and edge counts of the input and enhanced images for comparison. DV and BV is the average local variance of the foreground details and background respectively. The variance of each pixel is estimated using the gray-levels of the eight neighboring pixels over an entire image. From the variance image if pixels local variance is greater than the threshold then the variance of those pixels is the part of average foreground detail variance (DV), otherwise, the variance of those pixels is the part of average background variance (BV). In the case of an enhanced image the DV value increases, while the BV

value is not considerably changed compared to the original image, then contrast enhancement is realized. Also, a number of edges of the enhanced image are a comparison with the original image.

Finally, we examined the quality of the enhanced image based on the rate of identification performance of the proposed ear biometric system. Identification operation of the biometric system is evaluated on the basis of one-to-many comparison against all training samples to validate the identity of a test sample. The performance of the identification is measured using accuracy or correct identification or rate of identification, which is defined as the rate at which a number of samples are correctly classified out of total test samples. The rate of identification is measured in terms of ranks; rank-1 indicates the fraction of samples correctly classified based on first rank comparison results; similarly, rank-2 implies correct identification based on second rank comparison results and so on. The rate of correct identity of the probe samples within the top k ranks matching scores obtained from gallery samples is referred to as a rank- k identification rate. This is graphically represented using Cumulative Match Characteristic (CMC) curve, which evaluates the rank-wise cumulative sum of correct identification. Hence, it illustrates the rank in the x-axis and the cumulative rank accuracy in the y-axis.

Fig. 4 SURF keypoints matching for first and third rows with Poor contrast images and second and four rows with enhanced images



5.4 Analysis of numerical results

In this subsection, we discuss the experimental results of four different performance measures of HE, CLAHE, PSO, DE, and EJA based image enhancement approaches applied on the four above-mentioned ear image databases. These databases have low contrast, different lighting conditions, pose, and scale variation images. Figure 3 illustrates the

visual representation of the original images and EJA based enhanced images and their corresponding histograms on IITD, UND-E, UND-J2, and AWE databases. The Fig. 3 indicates the original images have narrow histograms and enhanced images have flat histograms. Consequently, the original low contrast image indicates one peak in the histogram and the original high contrast image indicates two peaks in the histogram of UND-E database sample image

Fig. 5 Four original images row-wise start from left to right enhanced gray-scale images using HE, CLAHE, PSO, DE, and proposed EJA enhancement techniques on IIT Delhi database

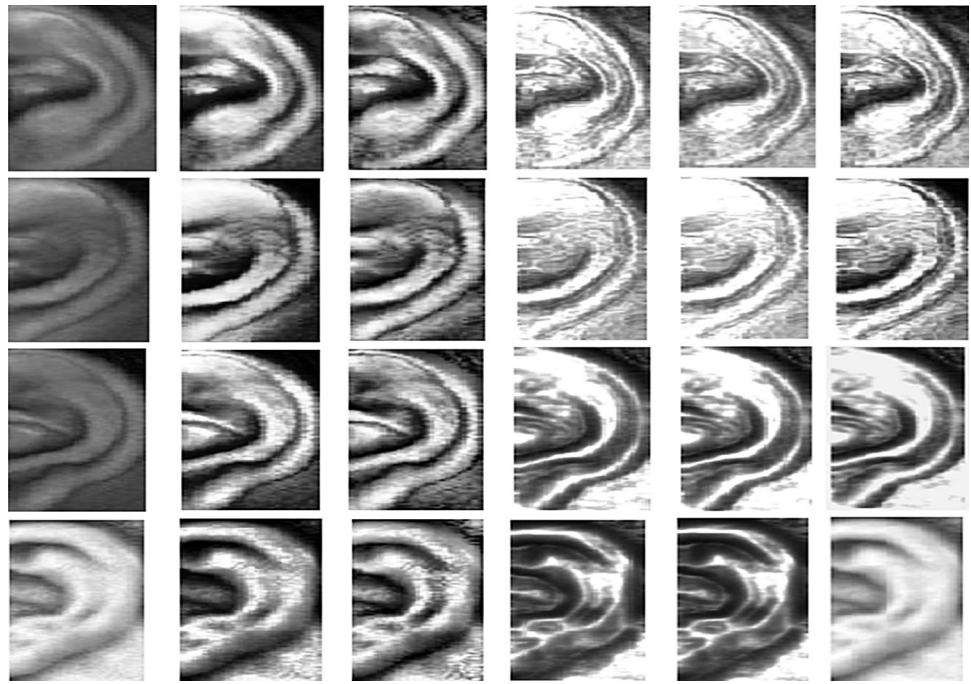


Fig. 6 Four original images row-wise from left to right enhanced gray-scale images using HE, CLAHE, PSO, DE, and proposed EJA enhancement techniques on UND-E database



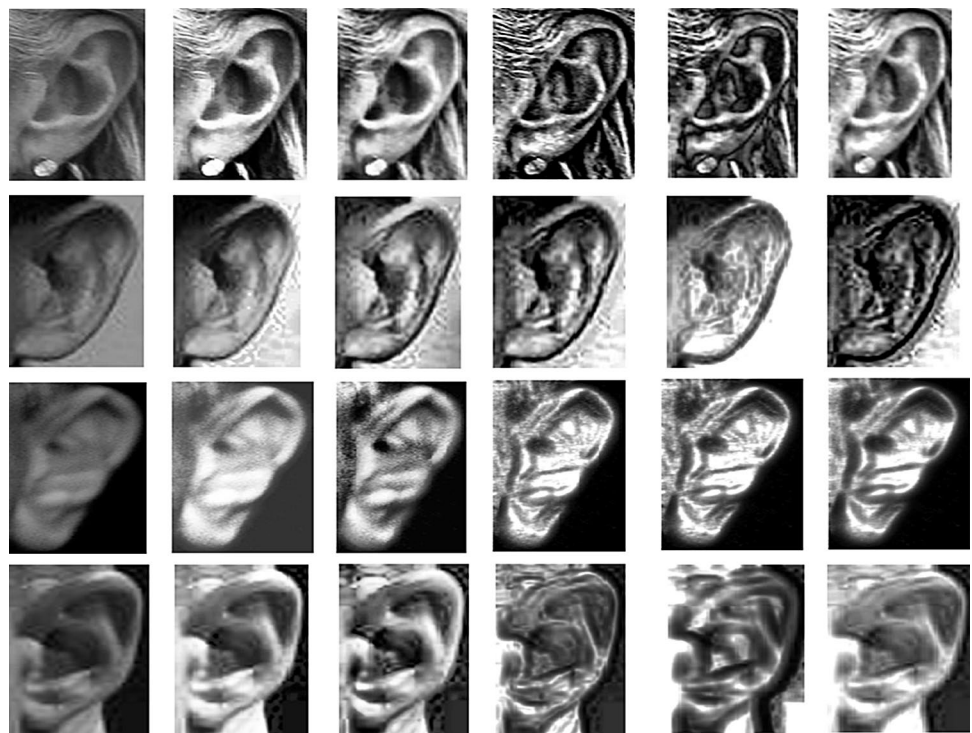
but their enhanced images have flat histogram. In addition, Fig. 4 presented the SURF feature key-points matching of original and enhanced images from the mentioned databases. It has found that if the enhanced image is not properly enhanced then it has less key-points matching. Tables 3, 3, 4 and 5 show the quantitative metrics such as

DV, BV, and edge count of original and enhanced images have been generated using HE, CLAHE, PSO, DE and proposed techniques on the mentioned databases. The quantitative measure of the edge count (EC) of all enhanced images on four mentioned databases, the proposed approach based enhancement produce have more edge counts than

Fig. 7 Four original images row-wise from left to right enhanced gray-scale images using HE, CLAHE, PSO, DE, and proposed EJA enhancement techniques on UND-J2 database



Fig. 8 Four original images row-wise from left to right enhanced gray-scale images using HE, CLAHE, PSO, DE, and proposed EJA enhancement techniques on AWE database



other mentioned enhancement approaches. However, in all four samples of IITD database DV values of HE-based enhancement have greater values than other enhancement techniques. Hence, it is clear that the performance HE-based enhancement performs better in IITD database than

other mentioned enhancement approaches. In other three databases, the proposed EJA-based enhancement approach provides better DV values in most of the sample images. Similarly, Tables 7, 8, 9 and 10 indicated an average rate of person identification using HE, CLAHE, PSO, DE, and EJA

Fig. 9 Identification rate curves of the proposed ear biometrics using HE, CLAHE, PSO, DE, and EJA on IITD database

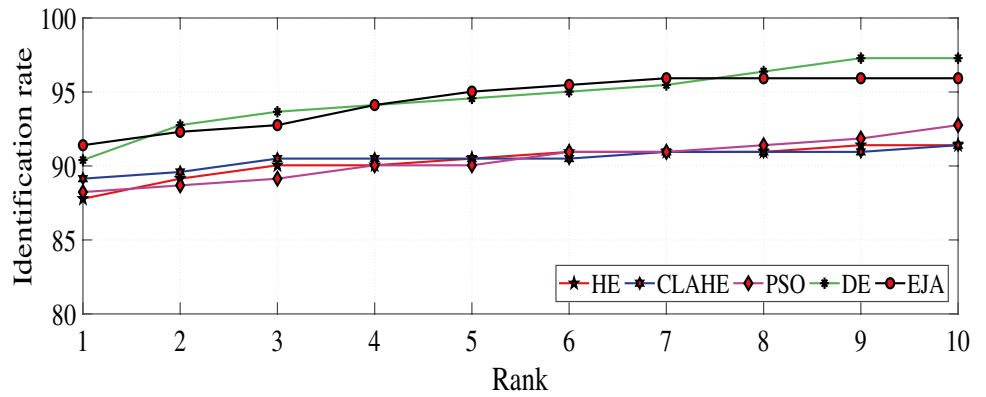


Fig. 10 Identification rate curves of the proposed ear biometrics using HE, CLAHE, PSO, DE, and EJA on UND (Collection E) database

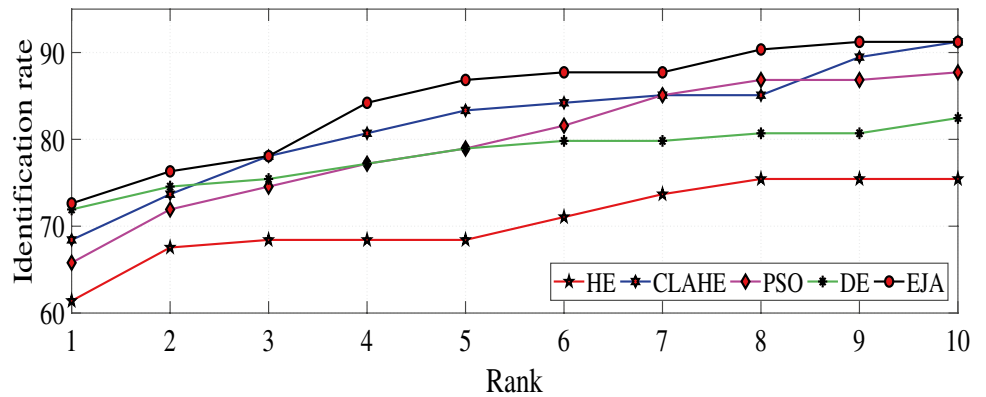
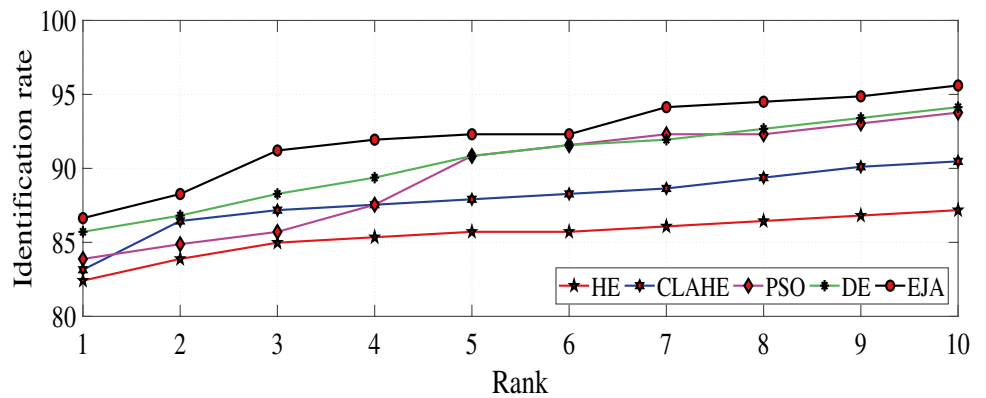


Fig. 11 Identification rate curves of the proposed ear biometrics using HE, CLAHE, PSO, DE, and EJA on UND (Collection J2) database



on the four mentioned databases. It is clearly observed that the proposed approach EJA outperforms over other techniques. As DE’s mutation operator has been used in EJA for more exploration and early convergence, which makes EJA rate of identification results slightly better than DE approach but EJA consumes less execution time in comparison to PSO and DE algorithm. In quantitative comparison based on person identification operation, we have taken two samples from each subject for training and one sample for testing in identification operation using different enhancement approaches at preprocessing stage in the ear

biometric system. In real world applications, we can increase the number of training samples per subject and employing dense local descriptors to represent ear images then the rate of identification ranks of proposed ear biometrics approach based on EJA image enhancement would be far better than the results have obtained in the experiments.

From the experimental results, it clearly observed, the proposed EJA approach is computationally faster and performance-wise efficient in case of illumination variation, low contrast, extraction of fine detail features, and presence of noise. It is also clear that the proposed approach is fully

Fig. 12 Identification rate curves of the proposed ear biometrics using HE, CLAHE, PSO, DE, and EJA on AWE database

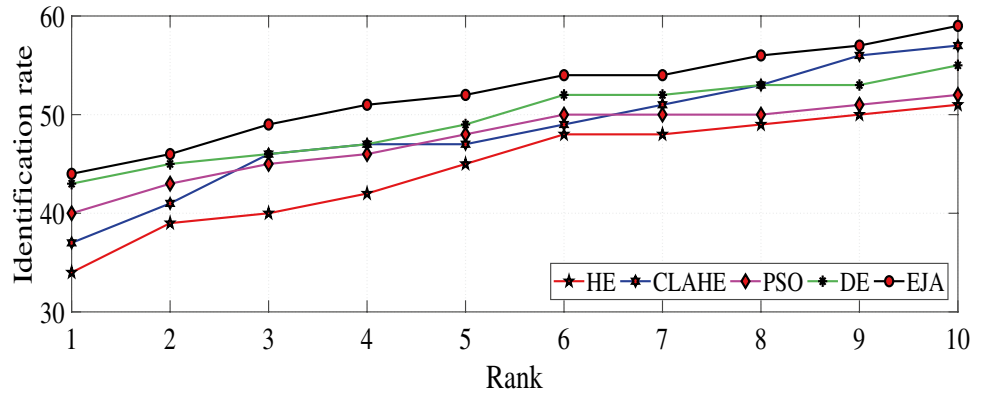


Table 3 Number of edge counts (EC), detail variance (DV) and background variance (BV) of the IITD database with nomenclature [Method name-Subject number-Image number]

Database image	DV	BV	EC
Original_040_1	0.167645	0.006696	246
HE_040_1	0.298301	0.006873	318
CLAHE_040_1	0.250168	0.005736	280
PSO_040_1	0.204537	0.005829	423
DE_040_1	0.208754	0.004822	395
EJA_040_1	0.203799	0.004989	97
Original_086_1	0.166281	0.005983	204
HE_086_1	0.303620	0.006929	317
CLAHE_086_1	0.242126	0.006989	266
PSO_086_1	0.199807	0.005654	427
DE_086_1	0.205634	0.003951	396
EJA_086_1	0.238101	0.005244	350
Original_120_2	0.166281	0.005983	204
HE_120_2	0.303620	0.006929	317
CLAHE_120_2	0.242126	0.006989	266
PSO_120_2	0.235318	0.004821	355
DE_086_1	0.003893	0.003893	397
EJA_120_2	0.204090	0.004271	400
Original_142_3	0.481217	0.005919	200
HE_142_3	0.362601	0.003052	198
CLAHE_142_3	0.335027	0.006058	221
PSO_142_3	0.267517	0.004224	337
DE_142_3	0.261184	0.004070	347
EJA_142_3	0.263690	0.004000	352

Table 4 Number of edge counts (EC), detail variance (DV) and background variance (BV) of the UND-E database with nomenclature [Method name-Subject number-Image number]

Database image	DV	BV	EC
Original-9-2	0.003872	0.003872	353
HE-9-2	0.368001	0.003486	512
CLAHE-9-2	0.347582	0.004632	516
PSO-9-2	0.405535	0.002191	665
DE-9-2	0.367844	0.005761	718
EJA-9-2	0.412613	0.002181	667
Original-32-1	0.466752	0.006295	359
HE-32-1	0.362474	0.003654	547
CLAHE-32-1	0.266633	0.006592	511
PSO-32-1	0.502376	0.006169	723
DE-32-1	0.244810	0.004630	432
EJA-32-1	0.239645	0.004556	438
Original-64-4	0.448097	0.005718	359
HE-64-4	0.359623	0.003271	404
CLAHE-64-4	0.336431	0.004141	439
PSO-64-4	0.435694	0.006673	514
DE-64-4	0.427487	0.006399	517
EJA-64-4	0.421637	0.006660	522
Original-9-2	0.351690	0.004135	312
HE-9-2	0.313107	0.006601	493
CLAHE-9-2	0.321950	0.006765	501
PSO-9-2	0.359173	0.005675	616
DE-9-2	0.385511	0.005173	623
EJA-9-2	0.404374	0.004826	643

automatic does not require parameters tuning for improving identification performance.

5.5 Computational execution time

In this section, we present the total average execution time of the proposed ear image enhancement using EJA and being compared with PSO and DE based ear image enhancement

approaches. According to Algorithm 1, the average execution time (T_{exe}) is sum of average time of three operations such as updating candidate solutions (T_{upd}), calculating fitness value for every candidate solutions (T_{fit}), and evaluating mutation (T_{mut}). The total time taken (T_{exec}) by the proposed approach as follows:

$$T_{exec} = T_{upd} + T_{fit} + T_{mut} \tag{21}$$

Table 5 Number of edge counts (EC), detail variance (DV) and background variance (BV) of the UND-J2 database with nomenclature [Method name-Subject number-Image number]

Database image	DV	BV	EC
Original-20-2	0.106253	0.005388	163
HE-20-2	0.357107	0.002965	242
CLAHE-20-2	0.245084	0.005465	205
PSO-20-2	0.457124	0.006840	270
DE-20-2	0.383312	0.006010	189
EJA-20-2	0.372988	0.006462	261
Original-72-2	0.078559	0.004772	196
HE-72-2	0.362690	0.003084	435
CLAHE-72-2	0.199160	0.005700	335
PSO-72-2	0.441229	0.007229	461
DE-72-2	0.301438	0.006999	462
EJA-72-2	0.298567	0.007027	470
Original-72-2	0.095220	0.004861	242
HE-72-2	0.356044	0.002727	409
CLAHE-72-2	0.217198	0.005320	379
PSO-72-2	0.408792	0.005373	275
DE-72-2	0.407284	0.006672	478
EJA-72-2	0.414617	0.006758	497
Original-72-2	0.167498	0.002198	239
HE-72-2	0.364460	0.002807	313
CLAHE-72-2	0.240268	0.004950	291
PSO-72-2	0.506332	0.002697	282
DE-72-2	0.478785	0.003274	524
EJA-72-2	0.478181	0.003255	523

Table 6 Number of edge counts (EC), detail variance (DV) and background variance (BV) of the AWE database with nomenclature [Method name-Subject number-Image number]

Database image	DV	BV	EC
Original-20-08	0.188705	0.006876	152
HE-20-08	0.301522	0.006131	198
CLAHE-20-08	0.278653	0.005392	184
PSO-20-08	0.250440	0.006632	170
DE-20-08	0.328728	0.005722	234
EJA-20-08	0.448370	0.004834	230
Original-42-05	0.423109	0.001617	198
HE-42-05	0.372765	0.002591	188
CLAHE-42-05	0.334818	0.005628	221
PSO-42-05	0.351148	0.003945	216
DE-42-05	0.399482	0.006094	240
EJA-42-05	0.382164	0.006380	227
Original-60-04	0.309747	0.006212	190
HE-60-04	0.277941	0.005536	206
CLAHE-60-04	0.428995	0.004002	207
PSO-60-04	0.222355	0.006589	214
DE-60-04	0.565369	0.004183	370
EJA-60-04	0.590189	0.005491	382
Original-100-09	0.103785	0.007353	163
HE-100-09	0.283432	0.007533	175
CLAHE-100-09	0.269048	0.005985	176
PSO-100-09	0.294041	0.006134	206
DE-100-09	0.320890	0.004934	231
EJA-100-09	0.367298	0.006775	284

In this work, we execute each approach 25 times to compute the average execution time. The experiments are implemented in MATLAB (R2017b) running on an Intel Core i5 PC with 2.6 GHz processor, 4 GB RAM, and Window 10 Operating System. For EJA, the average runtime for three operations (T_{upd}), (T_{fit}), and (T_{mut}) are computed to 0.017, 13.065, and 0.195 seconds respectively with the total execution time (T_{exce}) is 13.28 second. In EJA, adaptive mutation rate decides mutation operation. In the experiments, it has been observed that the average number of mutation operation is 26 out of 50 generations. However, mutation operator in DE is used for every generation and it takes 0.38 seconds which is approximately double as compared to the proposed EJA. Furthermore, two more operators (crossover and selection) of DE needs additional execution time as compared to the proposed EJA. Similarly, the average execution time of PSO based enhancement approach is very close to the proposed EJA due to slight difference in upgrading

candidate solutions. However, in PSO, first velocity of the birds (candidate solutions) is evaluated then the position of individual birds (candidate solution) is updated with respect to the velocity of individual birds. In EJA, positions of the candidate solutions are directly updated with the help of the current best and worst solutions. Table 11 indicates the average execution time in seconds for PSO, DE, and the proposed EJA based ear image enhancement approaches. It clearly indicates that execution time of the proposed EJA is less in comparison to classical PSO and DE based enhancement approaches. In terms of space complexity, EJA requires less memory space than other meta-heuristic optimization algorithms because it does not require any algorithm-specific parameters for tuning and directly upgrading the candidate solutions. Hence, the overall results reveal that the proposed EJA is an efficient image enhancement approach for the practical applications.

Table 7 Comparison of average identification rate of the proposed ear biometrics using HE, CLAHE, PSO, and DE on IITD database

Enhancement techniques	Average identification rate (%)	
	Rank-1	Rank-5
Histogram equalization (HE)		
Euclidean distance	87.33	94.57
Canberra distance	86.87	93.21
Nearest neighbor	82.8	90.95
CLAHE		
Euclidean distance	89.14	90.49
Canberra distance	72.85	76.27
Nearest neighbor	67.11	74.82
PSO		
Euclidean distance	88.23	90.04
Canberra distance	85.11	88.23
Nearest neighbor	80.13	78.43
DE		
Euclidean distance	90.04	95.5
Canberra distance	85.11	88.23
Nearest neighbor	80.13	78.43
Proposed EJA		
Euclidean distance	91.4	95.02
Canberra distance	85.11	88.23
Nearest neighbor	80.13	78.43

The bold value indicates the best average identification rate

6 Conclusion

In this paper, we proposed an ear biometric system by incorporating a new ear enhancement approach at the pre-processing stage using enhanced Jaya (EJA) meta-heuristic algorithm. The EJA introduces a mutation operator with the aim of faster convergence and improvement of the quality of ear images to enhance the performance of the ear biometric system. The proposed approach is tested with four benchmark databases from the literature. Computational results of the proposed enhancement technique are compared with two well-accepted conventional enhancement techniques such as histogram equalization, CLAHE, and two well-known meta-heuristic optimization like PSO and DE-based enhancement techniques. The qualitative and quantitative results based

Table 8 Comparison of average identification rate of the proposed ear biometrics using HE, CLAHE, PSO, and DE on UND-E database

Enhancement techniques	Average identification rate (%)	
	Rank-1	Rank-5
Histogram equalization (HE)		
Euclidean distance	61.4	66.66
Canberra distance	62.28	85.08
Nearest neighbor	64.91	80.7
CLAHE		
Euclidean distance	68.42	83.33
Canberra distance	64.03	84.21
Nearest neighbor	72.80	84.21
PSO		
Euclidean distance	70.47	82.94
Canberra distance	67.71	88.77
Nearest neighbor	71.22	92.38
DE		
Euclidean distance	71.92	85.94
Canberra distance	68.05	88.56
Nearest neighbor	70.22	95.87
Proposed EJA		
Euclidean distance	72.63	95.71
Canberra distance	68.71	89.77
Nearest neighbor	71.89	94.54

The bold value indicates the best average identification rate

on four databases clearly indicate the superiority of the proposed technique. It is also observed that proposed approach of image enhancement can be well-suited in the ear biometric system owing to the improved contrast of the original ear images that leads to extract more discriminative features in the feature extraction stage and subsequently increases the recognition performance.

There are some limitations that require future study. We can try other dense local feature descriptors instead of SURF with the expectation of improvement in the performance. Again, the proposed approach can also be improved by incorporating a multi-objective meta-heuristic optimization technique. Besides, another direction of research can be the use of deep learning based image enhancement approach in ear biometrics.

Table 9 Comparison of average identification rate of the proposed ear biometrics using HE, CLAHE, PSO, and DE on UND-J2 database

Enhancement techniques	Average identification rate (%)	
	Rank-1	Rank-5
Histogram equalization (HE)		
Euclidean distance	82.41	85.71
Canberra distance	79.48	89.01
Nearest neighbor	84.98	92.3
CLAHE		
Euclidean distance	83.15	87.91
Canberra distance	74.79	89.98
Nearest neighbor	78.72	90.15
PSO		
Euclidean distance	83.88	90.84
Canberra distance	80.95	92.67
Nearest neighbor	87.92	92.05
DE		
Euclidean distance	85.71	91.14
Canberra distance	83.74	90.88
Nearest neighbor	87.17	93.77
Proposed EJA		
Euclidean distance	86.64	92.85
Canberra distance	84.05	90.24
Nearest neighbor	88.72	92.33

The bold value indicates the best average identification rate

Table 10 Comparison of average identification rate of the proposed ear biometrics using HE, CLAHE, PSO, and DE on AWE database

Enhancement techniques	Average identification rate (%)	
	Rank-1	Rank-5
Histogram equalization (HE)		
Euclidean distance	34	45
Canberra distance	21	39
Nearest neighbor	17	21
CLAHE		
Euclidean distance	37	47
Canberra distance	22	40
Nearest neighbor	15	23.33
PSO		
Euclidean distance	40	48
Canberra distance	26	46
Nearest neighbor	26	44
DE		
Euclidean distance	43	49
Canberra distance	33	50
Nearest neighbor	28	42
Proposed EJA		
Euclidean distance	44	52
Canberra distance	32	52
Nearest neighbor	30	48

The bold value indicates the best average identification rate

Table 11 The average execution time (in seconds) achieved by the three meta-heuristic based ear image enhancement approaches

Algorithm	PSO	DE	EJA
CPU Time	14.47 ± 0.4	24.82 ± 1.4	13.28 ± 0.7

References

- Abate AF, Nappi M, Riccio D, Ricciardi S (2006) Ear recognition by means of a rotation invariant descriptor. In: 18th International conference on pattern recognition, ICPR 2006, vol 4, IEEE, pp 437–440
- Badrinath G, Gupta P (2009) Feature level fused ear biometric system. In: Seventh international conference on advances in pattern recognition, ICAPR '09, IEEE, pp 197–200
- Basit A, Shoaib M (2014) A human ear recognition method using nonlinear curvelet feature subspace. *Int J Comput Math* 91(3):616–624
- Bay H, Ess A, Tuytelaars T, Van Gool L (2008) Speeded-up robust features (surf). *Comput Vis Image Underst* 110(3):346–359
- Benzaoui A, Hadid A, Boukrouche A (2014) Ear biometric recognition using local texture descriptors. *J Electron Imaging* 23(5):053008
- Burge M, Burger W (2000) Ear biometrics in computer vision. In: 5th IEEE international conference on pattern recognition (ICPR)
- Bustard JD, Nixon MS (2010) Toward unconstrained ear recognition from two-dimensional images. *IEEE Trans Syst Man Cybern Part A Syst Hum* 40(3):486–494
- Chen Y, Zhang Y, Lu HM, Chen XQ, Li JW, Wang SH (2018) Wavelet energy entropy and linear regression classifier for detecting abnormal breasts. *Multimed Tools Appl* 77(3):3813–3832
- Choraś M (2005) Ear biometrics based on geometrical feature extraction. *Electron Lett Comput Vis Image Anal* 5(3):84–95
- Damer N, Führer B (2012) Ear recognition using multi-scale histogram of oriented gradients. In: 2012 Eighth international conference on intelligent information hiding and multimedia signal processing (IIH-MSP), IEEE, pp 21–24
- Das S, Suganthan PN (2011) Differential evolution: a survey of the state-of-the-art. *IEEE Trans Evolut Comput* 15(1):4–31
- Dhal KG, Ray S, Das A, Das S (2018) A survey on nature-inspired optimization algorithms and their application in image enhancement domain. *Arch Comput Methods Eng* 26(5):1607–1638
- Dodge S, Mounsef J, Karam L (2018) Unconstrained ear recognition using deep neural networks. *IET Biom* 7(3):207–214
- Elbes M, Alzubi S, Kanan T, Al-Fuqaha A, Hawashin B (2019) A survey on particle swarm optimization with emphasis on engineering and network applications. *Evolut Intell* 12(2):113–129
- Emeršič Ž, Križaj J, Štruc V, Peer P (2019) Deep ear recognition pipeline. In: Recent advances in computer vision, Springer, New York, pp 333–362
- Emeršič Ž, Štruc V, Peer P (2017) Ear recognition: more than a survey. *Neurocomputing* 255:26–39
- Emeršič Ž, Gabriel LL, Štruc V, Peer P (2018) Convolutional encoder-decoder networks for pixel-wise ear detection and segmentation. *IET Biom* 7(3):175–184
- Gorai A, Ghosh A (2009) Gray-level image enhancement by particle swarm optimization. In: 2009 World congress on nature and biologically inspired computing (NaBIC), IEEE, pp 72–77
- Guo Y, Xu Z (2008) Ear recognition using a new local matching approach. In: 15th IEEE International conference on image processing, ICIP 2008, IEEE, pp 289–292
- Hurley DJ, Nixon MS, Carter JN (2005) Force field feature extraction for ear biometrics. *Comput Vis Image Underst* 98(3):491–512

21. Iannarelli A (1989) Ear identification. Paramount Publishing, Hyderabad
22. Ibrahim MI, Nixon MS, Mahmoodi S (2010) Shaped wavelets for curvilinear structures for ear biometrics. In: Advances in visual computing, Springer, New York, pp 499–508
23. IIT Delhi Ear Database Version 1. http://web.iitd.ac.in/~biometrics/Database_Ear.htm
24. Islam SM, Bennamoun M, Davies R (2008) Fast and fully automatic ear detection using cascaded adaboost. In: IEEE workshop on applications of computer vision, WACV 2008, IEEE, pp 1–6
25. Kaiqi H, Zhenyang W, Qiao W (2005) Image enhancement based on the statistics of visual representation. *Image Vis Comput* 23(1):51–57
26. Kisku DR, Mehrotra H, Gupta P, Sing JK (2009) Sift-based ear recognition by fusion of detected keypoints from color similarity slice regions. In: International conference on advances in computational tools for engineering applications, ACTEA'09, IEEE, pp 380–385
27. Kumar A, Zhang D (2007) Ear authentication using log-gabor wavelets. In: International society for optics and photonics, defense and security symposium, pp 65390A–65390A
28. Mirjalili S (2019) Particle swarm optimisation. In: Evolutionary algorithms and neural networks, Springer, New York, pp 15–31
29. Nayak DR, Dash R, Majhi B (2018) Development of pathological brain detection system using jaya optimized improved extreme learning machine and orthogonal ripplelet-ii transform. *Multimed Tools Appl* 77(17):22705–22733
30. Pflug A, Paul PN, Busch C (2014) A comparative study on texture and surface descriptors for ear biometrics. In: 2014 International Carnahan conference on security technology (ICST), IEEE, pp 1–6
31. Prakash S, Gupta P (2012) An efficient ear localization technique. *Image Vis Comput* 30(1):38–50
32. Prakash S, Gupta P (2013) An efficient ear recognition technique invariant to illumination and pose. *Telecommun Syst* 52(3):1435–1448
33. Prakash S, Jayaraman U, Gupta P (2009) A skin-color and template based technique for automatic ear detection. In: Seventh international conference on advances in pattern recognition, ICAPR'09, IEEE, pp 213–216
34. Prakash S, Jayaraman U, Gupta P (2009) Ear localization using hierarchical clustering. In: International society for optics and photonics SPIE defense, security, and sensing, pp 730620–730620
35. Rao R (2016) Jaya: a simple and new optimization algorithm for solving constrained and unconstrained optimization problems. *Int J Ind Eng Comput* 7(1):19–34
36. Reza AM (2004) Realization of the contrast limited adaptive histogram equalization (clahe) for real-time image enhancement. *J VLSI Sig Proces Syst Sig Image Video Technol* 38(1):35–44
37. Sana A, Gupta P, Purkait R (2007) Ear biometrics: a new approach. *Adv Pattern Recognit* pp 46–50
38. Sarangi PP, Mishra B, Dehuri S (2017) Ear recognition using pyramid histogram of orientation gradients. In: 2017 4th International conference on signal processing and integrated networks (SPIN), IEEE, pp 590–595
39. Sarangi PP, Panda M, Mishra BP, Dehuri S (2016) An automated ear localization technique based on modified hausdorff distance. In: Proceedings of international conference on computer vision and image processing, Springer, New York, pp 229–240
40. Sarangi PP, Mishra BSP, Dehuri S (2018) Fusion of PHOG and LDP local descriptors for kernel-based ear biometric recognition. *Multimed Tools Appl* 78(8):9595–9623
41. Sarangi P, Mishra B, Majhi B, Dehuri S (2014) Gray-level image enhancement using differential evolution optimization algorithm. In: 2014 International conference on signal processing and integrated networks (SPIN), IEEE, pp 95–100
42. Solomon C, Breckon T (2011) Fundamentals of digital image processing: a practical approach with examples in matlab. Wiley, Hoboken
43. Storn R, Price K (1997) Differential evolution—a simple and efficient heuristic for global optimization over continuous spaces. *J Glob Optim* 11(4):341–359
44. Tiwari V, Jain S (2019) An optimal feature selection method for histopathology tissue image classification using adaptive Jaya algorithm. *Evolut Intell* 1–14
45. University of Notre Dame Ear Database, Collection E and Collection J2. <http://www.nd.edu/~cvrl/CVRL/DataSets.html>
46. Victor B, Bowyer K, Sarka S (2002) An evaluation of face and ear biometrics. In: 16th International conference and proceedings on pattern recognition, vol 1, IEEE, pp 429–432
47. Wang S, Rao RV, Chen P, Zhang Y, Liu A, Wei L (2017) Abnormal breast detection in mammogram images by feed-forward neural network trained by Jaya algorithm. *Fundam Inf* 151(1–4):191–211
48. Wang SH, Phillips P, Dong ZC, Zhang YD (2018) Intelligent facial emotion recognition based on stationary wavelet entropy and Jaya algorithm. *Neurocomputing* 272:668–676
49. Xie Z, Mu Z (2008) Ear recognition using LLE and IDLLE algorithm. In: 19th International conference on pattern recognition, ICPR 2008, IEEE, pp 1–4
50. Yuan L, Li C, Mu Z (2012) Ear recognition under partial occlusion based on sparse representation. In: 2012 International conference on system science and engineering (ICSSE), IEEE, pp 349–352
51. Yuan L, Mu ZC (2007) Ear detection based on skin-color and contour information. In: 2007 International conference on machine learning and cybernetics, vol 4, IEEE, pp 2213–2217
52. Zhang HJ, Mu ZC, Qu W, Liu LM, Zhang CY (2005) A novel approach for ear recognition based on ICA and RBF network. In: Proceedings of 2005 international conference on machine learning and cybernetics, vol 7, IEEE, pp 4511–4515
53. Zhang Y, Mu Z, Yuan L, Yu C (2018) Ear verification under uncontrolled conditions with convolutional neural networks. *IET Biom* 7(3):185–198

Publisher's Note Springer Nature remains neutral with regard to jurisdictional claims in published maps and institutional affiliations.